Supplementary Material (SM)

Nanoprobing of misfolding and interactions of amyloid β 42 protein

Bo-Hyun Kim[†,‡] and Yuri Lyubchenko[†,*]

[†]Department of Pharmaceutical Sciences, University of Nebraska Medical Center, 986025 Nebraska Medical Center, Omaha, NE 68198
[‡]Department of Materials Science and Engineering, KAIST, Daejon, Korea 305-701

Cysteine modified Aβ42

The white film of denatured Aβ42 cysteine modified at N-terminus was dissolved in DMSO (2 mg/ml) as a stock solution and then diluted to 1 μM in DMSO before use. The monomer state of Aβ42 diluted in different pH buffers from the stock solution was confirmed by the SDS-page gel experiment (Fig. S1). The gel was silver stained and over expressed (for more than 5 min) to visualize oligomers. Based on the intensity, the ratio of oligomers in the solution was estimated to be less than 7%.

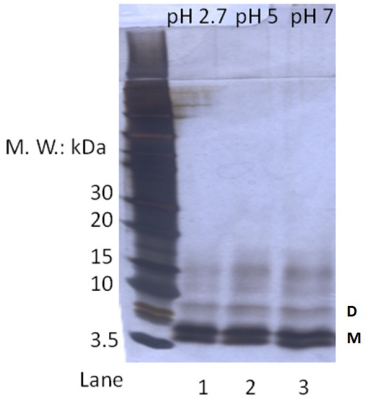

Figure S1. SDS-PAGE gel image of cysteine modified N-terminus of Aβ42(M.W.~4.6 kDa) dissolved in appropriate buffers with 20 μM TCEP. Left lane is the ladder of protein. Lanes 1-3 are the Cys-Aβ42 (4 μM) at pH 2.7, pH 5, and pH 7, respectively. M: monomer band, D: dimer band.

Surface density of the peptide immobilized via PEG linkers

The surface density of Aβ peptide was estimated from the surface AFM images of α-synuclein

(α-Syn) using dsDNA with 42 base-pair and the protocol described in [1, 2]. Here we used thiolated DNA duplexes capable of covalent binding to maleimide groups on mica substrate to evaluate the binding efficiency of MAS-surfaces. DNA duplexes were fluorescently labeled to measure the efficiency of DNA binding in parallel to the AFM imaging. Fluorescence dye labeled oligonucleotide and its complementary were synthesized (IDT, Coralville, IA). The sequences are as follows:

Y18O2: 5'-ACC TAA CCG GAA A/iAmMC6T/T ACG AGA AAT AGA TGC ATG CAA GCT TCA CA-3'

ComY18O2: 5'ThioMC6-D-TTTTTTTTTTTG TGA AGC TTG CAT GCA TCT ATT TCT CGT AAT TTC CGG TTA GGT -3'

The first oligonucleotide was labeled with succinimide esters of Cy5 dye (Amersham Pharmacia Biosciences) according to the protocol provided. Labeled oligonucleotide was purified by RP-HPLC using a Matrix Polystyrene/divinyl benzene column (5 RPC ST 4.6/150, Amersham Pharmacia Biotech). dsDNA was prepared by mixing two oligonucleotides each with 4 μM concentration in Tris-EDTA (10 mM/1 mM) with NaCl (150 mM) buffer (pH 7.4), and then by repeating the annealing process (0.5 °C/min from 50 °C to 90 °C) two times. Fig. S2 is the melting curves of duplexed oligonucleotides, which shows the melting temperature of 76.23 ± 0.78 °C (Inset).

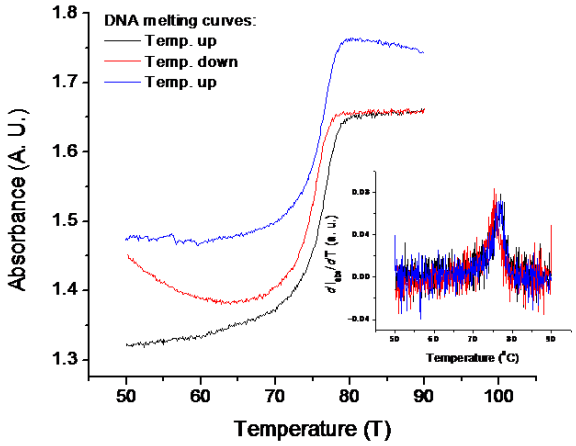

Figure.S2. Melting curves measured from 50 °C to 90 °C with the rate of 0.5°C/min. The tail appearing in the temperature down curve originated from the evaporation of buffer during the process. Inset. Differential curves of measured melting curves. The peak indicating the melting temperature was located at 76.23 ± 0.78 °C.

The yield of the duplexed DNA determined by gel electrophoresis (Fig. S3) was ~85%. DNA duplexes were incubated with MAS modified glass and mica surfaces. However, in AFM images the dsDNA molecules appear as dots (Fig. S4). The dot size was 10~20 nm of length and 1~1.5

nm of height. The surface density of incorporated dsDNA evaluated from AFM images was less than 1/(180x180) nm^2, suggesting that the surface is sparsely modified justifying the single molecule probing regime for the force probing.

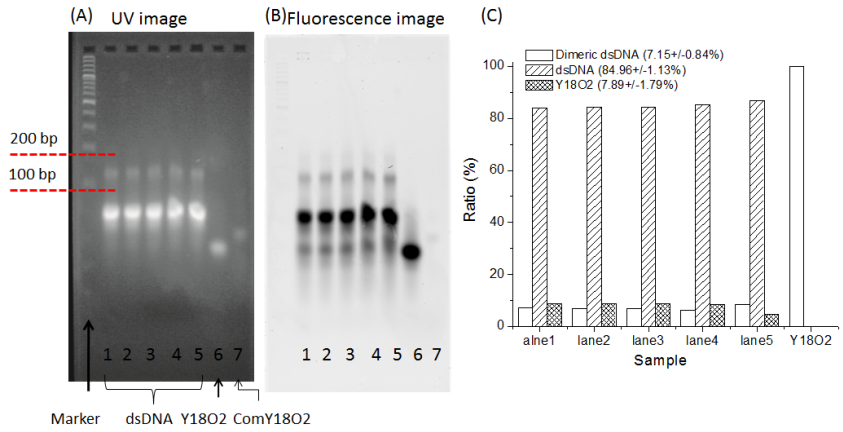

Figure S3. Gel electrophoresis data of dsDNA used for testing of MAS-mica surface. Agarose gel (2.5%) of annealed dsDNA (lane 1~5) and two oligonucleotides (lane 5: Y18O2, land 6: ComY18O2) before coupling stained with ethidium bromide (A) and Cy5 fluorophore (B) in which labeled DNA and Y18O2 appear as black bands, whereas ComY18O2 (lane 7) is very faint. (C) Quantitative analysis of the data in (B). Based on the fluorescence intensity of gel images, the yield of labeling is ~85± 1.1 %.

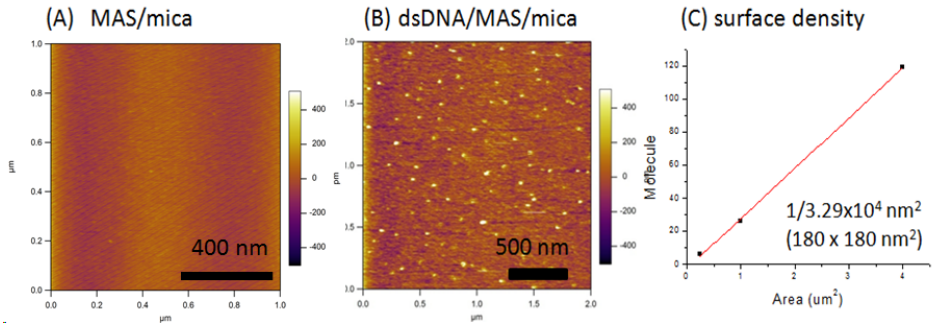

Figure S4. AFM images and surface density graph. (A) Control surface: MAS modified mica surface (B) dsDNA immobilized MAS/mica surface. dsDNAs were imaged as white dots, which had height of 1~1.5 nm and length of 10~20 nm. (C) The graph shows the number of dsDNA vs. the size of the scanned area.

Statistical analysis of F-D curves

Multiple independent experiments were performed at both pH values and the data were averaged

over these independent measurements. Table below shows the results of force distribution obtained in such experiments. The values obtained in independent experiments well overlay. The mean values were obtained from the averaging over this set of measurements and shown in the table.

Table S1. The rupture force values for five independent probing experiments performed at two pH values. The mean values and the errors are shown in the last column.

	Exp. 1	Exp. 2	Exp. 3	Exp. 4	Exp. 5
pH 7	91.7 (±23.2)	63.1 (±24.6)	80.5 (±14.2)	71.0 (±19.0)	77.3 (±11.6)
pH 2.7	86.2 (±13.4)	80.1 (±24.4)	62.1 (±15.1)	63.6 (±14.4)	80.8 (±24.6)

Persistence length distribution

Figure S5 shows the histogram of persistence length distributions obtained from the force-distance curves which were fitted by the WLC model. The Gaussian fitted histogram showed that the distribution of the persistence lengths measured at pH 7 and 2.7 has a mean value (± SD) of 0.2 ± 0.1 nm and 0.14 ± 0.07 nm.

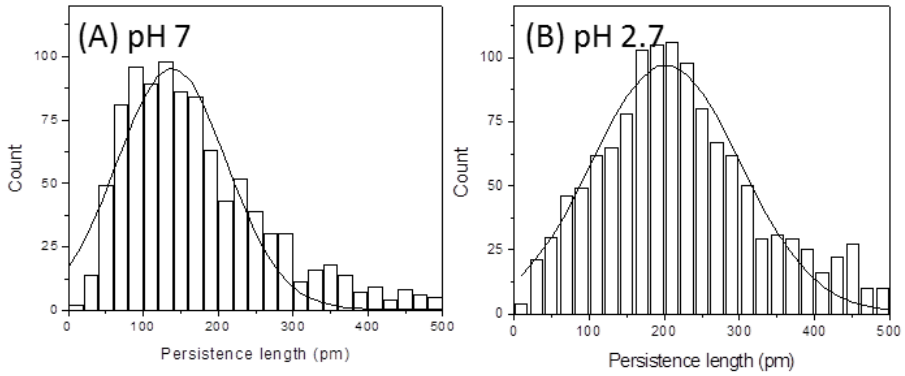

Figure S5. Histograms of the distribution of persistence lengths for pH 7 (A) and 2.7 (B). Solid line in histograms are the Gaussians.

Rupture force dependence on the loading rate

Figure S6 shows the representative force curves with different rupture forces corresponding to different loading rates. Force curve (A) was measured at a loading rate of 100 nm/s, and (B~E) were measured at 200 nm/s, 500 nm/s 1 μm/s, and 3 μm/s, respectively. The rupture force for each curve was ~50 pN, ~80 pN, ~170 pN, ~220 pN, and ~310 pN for curves (A-E), respectively.

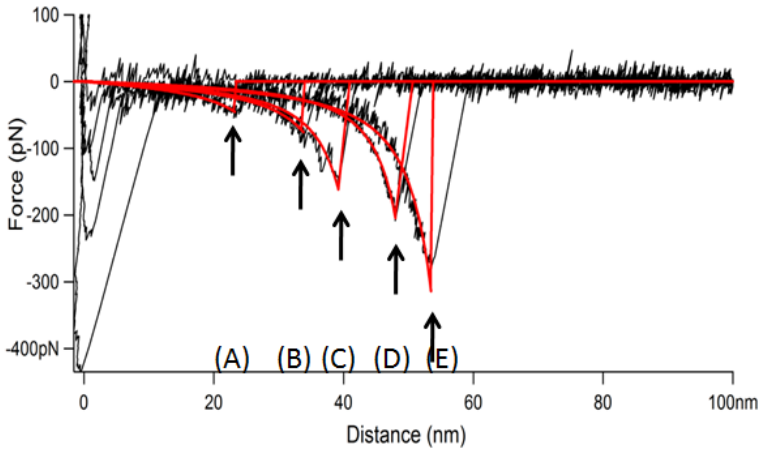

Figure S6. Representative force curves with different rupture forces according to the loading rate.

Control force spectroscopy experiments

Figure S7 shows the results of control experiments measured in four different pulling rates, 100 nm, 400 nm, 1 μm, and 3 μm. The results for the control experiment without Aβ42 in both tip and substrate are shown in Fig. S7A. Figure S7B demonstrates the result of control experiment with Aβ42 in either tip or substrate. The non-specific rupture event ratio for each control experiment was ~1.6% and ~1.1%, respectively.

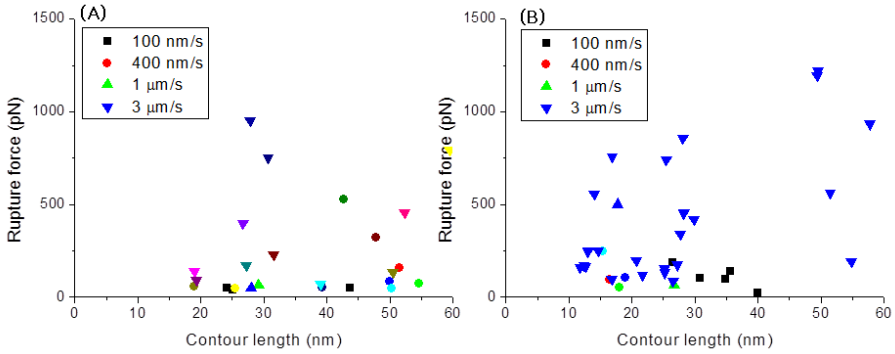

Figure S7. Control experiments for the system without Aβ42 in both tip and substrate(A) and from the system with Aβ42 in either tip or substrate (B).

The contour length measurements – effects of loading rate and PEG polydispersity

Figure S8 shows theoretical dependence of the PEG contour length on the rupture force for three lengths of PEG calculated using the extended Langevin function.[3] The range of the contour lengths was defined by the polydispersity of PEG linker used in the experiments [2, 4]. This graph shows that the contribution to the contour length from the force dependence of PEG is less than 7%

in the range of 50 pN and 120 pN of rupture forces. The polydispersity of PEG was measured by mass spectroscopy and NMR [2, 4].

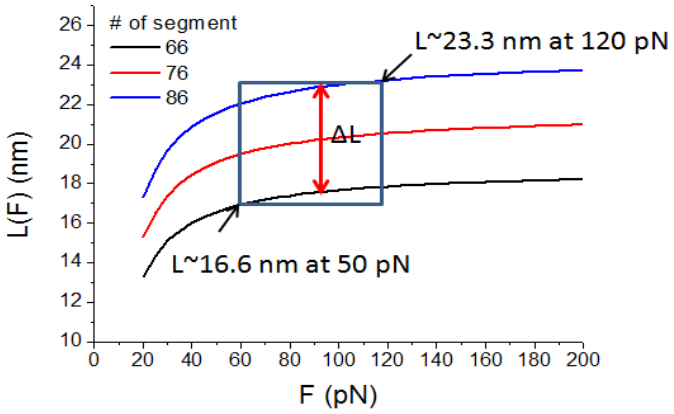

Figure S8. The dependence of the PEG contour length on the pulling force calculated using analytical equation of the extended Langevin function. Different colors were used for the PEG polymers with different lengths.

References

1. Lyubchenko YL, Kim BH, Krasnoslobodtsev AV, Yu J. Nanoimaging for protein misfolding diseases. Wiley Interdiscip Rev Nanomed Nanobiotechnol. 2010;2(5):526-43.

2. Yu J, Warnke J, Lyubchenko YL. Nanoprobing of alpha-synuclein misfolding and aggregation with atomic force microscopy. Nanomedicine. 2010.

3. Oesterhelt F, Rief M, Gaub HE. Single molecule force spectroscopy by AFM indicates helical structure of poly(ethylene-glycol) in water. J New Journal of Physics. 1999;1.

4. Kim BH, Palermo NY, Lovas S, Zaikova T, Keana JF, Lyubchenko YL. Single-Molecule Atomic Force Microscopy Force Spectroscopy Study of Abeta-40 Interactions. Biochemistry. 2011.